Composites: Part A 184 (2024) 108273

Contents lists available at ScienceDirect

Composites Part A

journal homepage: www.elsevier.com/locate/compositesa

Double percolation approach for hybrid graphene Nanoplatelet-Carbon black nanocomposites based on electrical impedance Spectroscopy

X.F. Sánchez-Romate [a,*], A. Jiménez-Suárez [a], J.M. Sanz-Ayet [a], V. García-Martínez [b], M.R. Gude [b], S.G. Prolongo [a]

[a] Materials Science and Engineering Area, Escuela Superior de Ciencias Experimentales y Tecnología, Universidad Rey Juan Carlos, Calle Tulipán s/n, 28933 Móstoles (Madrid), Spain

[b] FIDAMC, Foundation for the Research, Development and Application of Composite Materials, Avda. Rita Levi-Montalcini 29, 28906 Getafe, Madrid, Spain

ARTICLE INFO

Keywords:
Nano-structures
Electrical properties
Analytical Modelling
Electron microscopy

ABSTRACT

A double-percolation model for predicting electrical properties in hybrid carbon black (CB)-graphene nanoplatelet (GNP) nanocomposites is proposed. This model is based on DC and EIS measurements. From DC measurements, a non-ohmic behavior is observed for low-filled nanocomposites whereas at high-filled ones, an ohmic behavior is noticed. From EIS analysis, the behavior of the system can be modeled by an equivalent circuit formed by a series of inductance-resistance capacitance (LRC), for contact and intrinsic electrical mechanisms, and resistance–capacitance (RC) elements, for tunneling transport, where the capacitances are substituted by Constant Phase Elements (CPEs) due to the presence of scattering effects. The complex impedance analysis shows a GNP-dominated electrical behavior at a high CB/GNP ratio. At a medium CB/GNP ratio a double percolating network is formed. At a low CB/GNP ratio, the electrical transport is CB-dominated. The proposed model based on the classical percolation theory with a double threshold properly fits the electrical measurements.

1. Introduction

In recent decades, there has been an increasing interest in the use of carbon nanoparticles such as carbon black (CB), carbon nanotubes (CNTs), or graphene nanoplatelets (GNPs) due to their exceptional mechanical, electrical, and thermal properties [1,2].

In this sense, the use of hybrid carbon nanofillers is also gaining interest, as it is possible to achieve synergistic properties in this way. For example, it has been reported that the addition of a very small amount of hybrid CNT-GNP nanofillers may lead to an enhanced electrical network with superior electrical properties [3,4]. Similar behavior is observed in hybrid CB-CNT nanocomposites, where a synergistic effect is observed in terms of electrical conductivity when adding a small content of CBs to the CNT electrical network [5,6]. The use of hybrid nanofillers has proved to be an effective way to enhance, for example, the strain-sensing behavior of the system indeed [7,8]. Here, it is important to understand in a detailed way the electrical transport mechanisms to achieve the best properties depending upon the application.

To date, there are a lot of analytical and numerical models dealing with different effects such as nanoparticle orientation, aggregate distribution, or waviness for single-filled nanocomposites such as CNT [9–12], GNP [13] or CB-based ones [14]. In addition, other studies present theoretical models adaptable to different nano- and microfillers taking various aspects into account such as the geometry of the nanofiller, aspect ratio, dispersion method, etc. [15]. However, the electrical transport mechanisms in hybrid nanocomposites are quite hard to understand and model.

In this regard, theoretical approaches have been developed for different hybrid systems such as CNT-carbon nanofibers (CNFs), where the effect of nanofiller alignment has been proved to be a critical factor for predicting the electrical conductivity of the system [16]. Moreover, some studies explored the piezoresistive properties of CNT-CB nanocomposites [17,18]. Others reported the electrical and piezoresistive properties of GNP-CNT nanocomposites using analytical modeling and Monte Carlo simulations [19,20]. However, most of these studies involve the use of complex models and statistical tools and often fail to give a simple overview of electrical transport mechanisms in this type of materials, as they suppose random distribution of nanoparticles which, in most cases, is not the real situation.

For this reason, this work aims to explore a different approach to

* Corresponding author.
E-mail address: xoan.fernandez.sanchezromate@urjc.es (X.F. Sánchez-Romate).

https://doi.org/10.1016/j.compositesa.2024.108273
Received 8 March 2024; Received in revised form 17 March 2024; Accepted 16 May 2024
Available online 18 May 2024

thoroughly understanding electrical transport mechanisms. Some studies have dealt with the development of a simple theoretical approach to model the electrical percolating network in a hybrid nanocomposite. For example, M. Haghgoo et al. [21] developed a tunneling-assisted model for hybrid CNT/chopped carbon fibers (CF) composites Furthermore, Y. Sun et al. [22] proposed a simple theoretical approach to estimate the percolation threshold, that is, the critical volume fraction where the polymer becomes electrically conductive, of hybrid CNT-CB nanocomposites, then modified by Z.Y. Xiong et al [23] to take some parameters such as the nanofiller aspect ratio into account in polymer blends with hybrid CNT-CB nanofillers. However, depending on the dispersion procedure and, thus, on the electrical network created, which can be sometimes very complex, this simple model may not predict the electrical behavior effectively [24]. Here, in some cases, CNTs or CB will form dead networks due to the interconnections between CNT branches or CNTs and CB, as proposed by J. Sumfleth et al. [25] and, thus, it is necessary to deeply explore the electrical properties and transport mechanisms in this type of materials. For these reasons, this study aims to develop a simple model that properly reflects these electrical transport mechanisms, as well as the possible interconnections between the nanofillers for hybrid nanocomposites formed with GNPs and CBs in an epoxy matrix.

To achieve this purpose, first, DC electrical conductivity measurements have been carried out, as the I-V characteristic curves can give an initial approach to the electrical properties of these systems. However, they do not give a detailed approach to the main electrical transport mechanisms. In this sense, the analysis of the electrical impedance behavior will be more useful.

AC measurements have been used to characterize the frequency-dependent behavior of the electrical conductivity as a function of nanofiller content in carbon-based nanocomposites [26,27] and, even, for the determination of the electrical properties of carbon fibers [28]. Furthermore, Electrical Impedance Spectroscopy (EIS) has been also used in other studies as a technique for determining the main electrical transport mechanisms in CNT [29] and GNP [30] nanocomposites, separately. Here, the electrical impedance response can be fitted by a simple equivalent circuit that properly captures these transport mechanisms between nanoparticles.

In this work, the main goal is to adapt this EIS analysis to hybrid CB-GNP nanocomposites for a better understanding of the electrical properties. More specifically, a correlation between the electrical impedance behavior and the classical percolation theory adapted to hybrid nanofillers will be carried out. Here, the agreement between the measured data and the theoretical predictions would validate the proposed model.

The main novelty of the present work lies in the fact that there are no papers reporting the EIS behaviour of these systems (GNP-CB) by using an equivalent electrical circuit for modelling the electrical behaviour.

More specifically, the use of equivalent circuit for modelling the electrical response has been reported in previous studies [29,30], as commented before, but only for GNP or CNT-based nanocomposites, so the investigation of this type of electrical modelling remains unexplored for hybrid nanofillers.

Here, with the incorporation of this electrical model, it would be very easy to understand the governing electrical transport mechanisms in GNP-CB based nanocomposites. The incorporation of the double percolation mechanism has been proved in polymer blends reinforced with single filler (CB, CNT or GNP) [31,32], but their incorporation for predicting the electrical conductivity of hybrid-nanofiller remains unexplored. By using this simple approach, it would be possible to estimate the precise contribution of the two nanofillers having a much more detailed knowledge of the material.

In this way, it would be possible to better understand the main transport mechanisms in a simple but effective way, which would be a first step for the fabrication of hybrid nanocomposites with tunable properties.

2. Experimental

2.1. Materials

The epoxy resin was a mono-component low-viscosity resin recommended for Resin Transfer Moulding (RTM), with a commercial formula called *HexFlow RTM 6, based on* diglycidyl ether of bisphenol (DGEBA) cured with aromatic amines, supplied by *Hexcel*.

Two types of nanofillers were used: carbon black (CB) and graphene nanoplatelets (GNPs). CBs were supplied by *Songhan Imerys* with the commercial name *Ensaco 250G*, with a BET surface area of 65 m2/g and a density of 0.17 g/cm3. GNPs were commercially named *M25*, supplied by *XG Sciences*, with an average lateral size of 25 μm, a thickness of 6–10 nm, and a density of 2.2 g/cm^3.

2.2. Manufacturing of CB-GNP nanocomposites

The manufacturing of CB-GNP nanocomposites followed three steps: (1) dispersion of the nanofiller, (2) degasification step, and (3) curing process.

The nanofillers dispersion in turn followed two different techniques. In the case of CB-based nanocomposites, the nanofillers were dispersed by toroidal stirring using a *Dispermat* dissolver at 6000 rpm with a rotating disc of 50 mm diameter for 15 min. The reason for the use of toroidal stirring, in this case, is justified as it is highly scalable and allows the fabrication of large batches. However, it is not a proper technique for the dispersion of GNPs. For this reason, in the case of GNP-based nanocomposites, the nanoplatelets were dispersed by a three-roll-milling process using a single cycle of a 40 μm gap between rolls at a rotating speed of 250 rpm. This single calendering cycle was selected to avoid the breakage of the nanoplatelets, as proved in a previous study [33].

In the case of hybrid nanocomposites, first, the CBs were dispersed by toroidal stirring in a single batch containing 11 wt% of nanoparticles for 15 min. Then, the resin and the GNPs were added to get the desired concentration and they were dispersed using the previously commented single cycle of three-roll-milling.

After dispersion, the resulting mixture was degassed at 90 °C at vacuum conditions for, at least, 15 min to remove the possible entrapped air, and, after degasification, it was poured into a metallic mold that was previously prepared with a liquid demolding agent *Frekote* and cured with an isothermal cycle at 180 °C during 120 min in a convection oven. Table 1 summarizes the different nanocomposites fabricated and Fig. 1 shows a schematic of the manufacturing process. It is important to point out that no further nanofiller contents were explored due to the extremely high viscosity of the mixture, which difficulted the proper processing.

Table 1
. Summary of designations and conditions manufactured.

Designation	GNP content (wt.%)	CB content (wt.%)
G-1	1	–
G-2	2	–
G-3	3	–
CB-3	–	3
CB-5	–	5
CB-8	–	8
CB-11	–	11
CB3-G1	1	3
CB3-G2	2	3
CB3-G3	3	3
CB5-G1	1	5
CB5-G2	2	5
CB5-G3	3	5

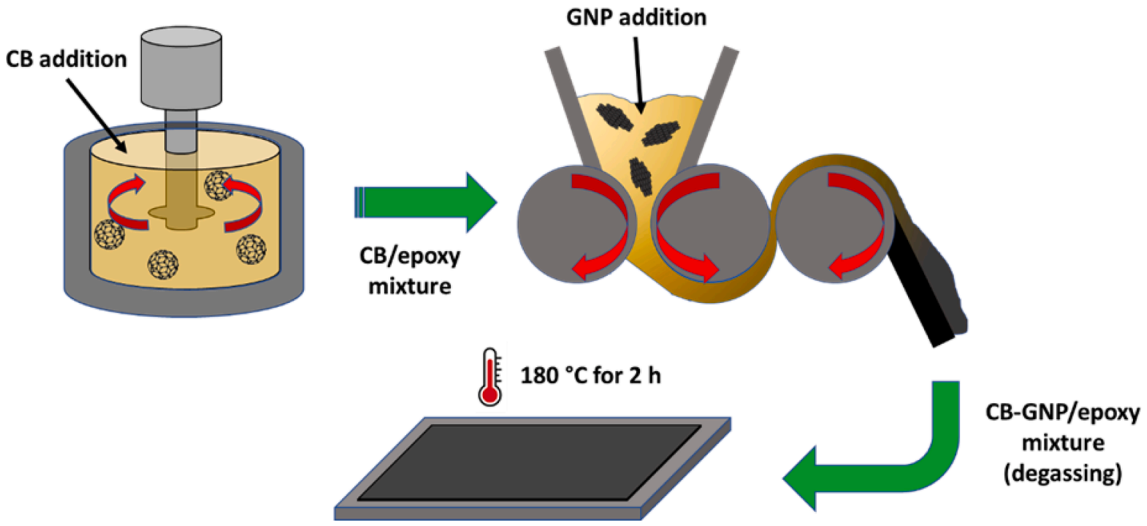

Fig. 1. Schematics of dispersion procedure of CB-GNP nanocomposites.

2.3. Microstructural characterization

Microstructural characterization was carried out using a Field Emission Gun-Scanning Electron Microscope (FEG-SEM) *Nova NanoSEM FEI 230* from Philips. Transversal sections of fractured materials were characterized. This fracture was conducted under cryogenic conditions to create a smooth surface and a 3.1 nm thickness Pt layer was deposited by sputtering on the surface before observation. The aim was to properly observe the nanofiller distribution in the final nanocomposites.

2.4. Electrical characterization

Electrical characterization was carried out through DC measurements and EIS analysis. DC volume conductivity was evaluated according to ASTM D257 using a *Source Measurement Unit (SUM)* of Keithley Instrument Inc. (mod. 2410) connecting through an interface GPIB to a PC. I-V characteristics curves were obtained for each condition using 5 samples of 10 × 10 × 1 mm. Silver paint was used to ensure good contact with the electrodes of the 10 × 1 mm section. The voltage range was set at 0–200 V for every condition.

EIS analysis was conducted in, at least, two samples of 30 × 10 × 3 mm for each conductive condition. The measurements were done in an *AUTOLAB PGSTAT302 N* potentiostat at a frequency range of 0.1–10^5 Hz and a voltage amplitude of 30 mV at room temperature conditions. Two copper wires attached with silver ink to the nanocomposite surface were used as electrodes. The adjustment of the measured data with electrical circuits was carried out by *Nova 2.1* software.

3. Results and discussion

In this section, first, an analysis of DC measurements is carried out to gain first knowledge about the electrical properties of the nanocomposites. Then, a detailed analysis of electrical transport mechanisms by complex impedance measurements is conducted, with an equivalent circuit modeling. Finally, a connection between DC measurements and electrical impedance performance is proposed by a simple analytical model based on a double-percolation theory.

3.1. Analysis of DC measurements

Fig. 2 summarizes the I-V curves for the GNP, CB, and hybrid CB-GNP nanocomposites. It is important to point out that there is not a linear correlation between the applied voltage and the current in some conditions. This non-ohmic behavior has been observed in many studies based on graphitic nanofilled nanocomposites [34–36].

More specifically, a linear-exponential correlation can be found between the applied voltage, *V,* and the current flow through the nanocomposite, *I* [37]:

$$I = GVexp(kV) \tag{1}$$

where *G* is the conductance at 0 V and *k* is a fitting parameter. A higher value of *k* denotes a more prevalent exponential behavior.

In addition, the electrical conductivity at 0 V can be estimated from the conductance and the geometry of the sample:

$$\sigma_0 = \frac{GL}{A} \tag{2}$$

Being L and A the length between the electrodes and the electrode contact area, respectively.

In this sense, Fig. 2e and f show the values of fitting parameters for the different conditions. It is important to point out that the samples with only 3, 5, and 8 wt% CB showed a conductivity below the range of the multimeter, so they will be considered non-electrically conductive, that is, they do not form electrical percolating networks.

It can be observed that, generally, the values of the *k* parameter decrease with increasing the nanofiller content. The non-ohmic behavior is explained because, when increasing the applied voltage, a temperature increase is observed due to the heat dissipation by Joule's effect [38,39]. This temperature increase will affect the main electrical transport mechanisms inside the graphitic network and, thus, the electrical conductivity will change. For this reason, a linear relationship between applied voltage and current could not be observed.

More specifically, it can be elucidated that there is a more prevalent exponential correlation between the voltage and the current of low-filled nanocomposites with a high value of *k*. This is explained because, at low nanofiller contents, the electrical transport mechanisms are more dominated by the matrix, which usually exhibits a positive dependence on the electrical conductivity with temperature [40]. However, when increasing the nanofiller contents, there is more prevalence of contact mechanisms between adjacent nanoparticles, and, therefore, the collision between the free electrons and the carbon atoms in the graphitic nanofillers would become more probable [41]. For this reason, when increasing the nanofiller content, a less prevalent increase of the electrical conductivity with temperature is observed, even a reduction [42]. This would be reflected, thus, in a detriment of the *k* parameter, as observed.

Furthermore, when analyzing the values of σ_0, it can be noticed that, for the neat GNP and CB-only doped samples, it increases with nanofiller

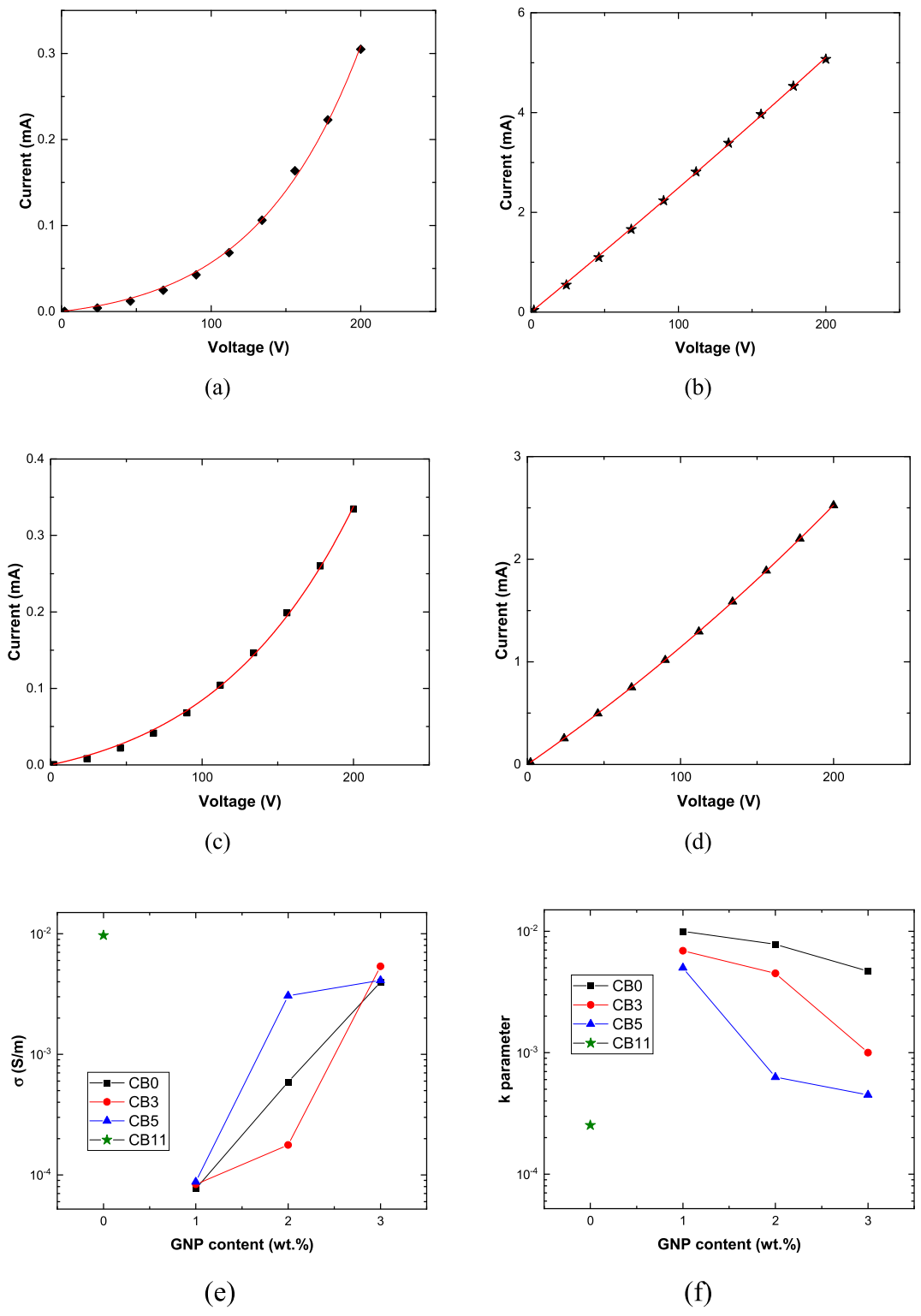

Fig. 2. Representative I-V curves of (a) G1, (b) CB11, (c) CB-3G1 and (d) CB3-G3 samples, where the dots represent the measurements and the solid line (in red) the fitting by Equation (1) (the rest of I-V curves can be found in Fig. S1), and (e) electrical conductivity at 0 V and (f) values of *k* parameter (the precise values can be found in Table S1).

content, as expected, due to the presence of more conductive electrical pathways that lead to the creation of more efficient electrical networks. However, in the case of CB-GNP hybrid nanocomposites, the evolution of this parameter is quite more complex. For a fixed CB content, it is observed that it increases with GNP content, as there are more connections between CB and GNPs and, thus, there are more electrical pathways inside the nanocomposite. However, when comparing the 3 wt % CB and 5 wt% CB-based hybrid nanocomposites, the differences between σ_0 are very low. This can be explained because the 5 wt% CB hybrid nanocomposites present a more aggregated distribution of nanoparticles, especially in the case of CBs, being the presence and size of agglomerates much more prevalent than in the case of 3 wt% CB

nanocomposites (Fig. 3a and b).

This highly inefficient electrical network can be explained by the effectiveness of the dispersion procedure. As a general fact, although toroidal stirring is a technique that promotes a high homogenization of the nanofillers, it is a much less aggressive dispersion technique than three-roll-milling, and, for this reason, in the case of a highly viscous mixture, the size of the agglomerates will be higher [10]. Therefore, the incorporation of GNPs with the three-roll-milling process will be less efficient in highly CB-filled composites and, thus, the enhancement of the electrical conductivity will be less significant.

The analysis of DC measurements may offer a global overview of the electrical properties, but they do not give detailed information about the dominant electrical transport mechanisms, specifically, in hybrid nanofilled composites. For this reason, a detailed analysis of the electrical impedance behavior will be carried out.

3.2. Electrical impedance analysis

Fig. 4 shows the Nyquist plots (real, Z', versus imaginary part, −Z'', of the complex impedance) for the different nanocomposites. It can be observed that the shape of the Nyquist plots is quite different when comparing pure GNP and CB nanocomposites. In the case of GNP-based composites, a wide semicircle is observed (Fig. 4a), whereas, in the case of CB-based ones, two semicircles are observed (Fig. 4b). This would denote that the electrical transport mechanisms are different depending on the nanofiller used. In addition, when comparing the CB-GNP hybrid composites, a change in the electrical impedance behavior is observed when varying the GNP to CB ratio, denoting a prevalence of GNP-type or CB-type transport mechanisms depending on the proportion of each constituent (Fig. 4c-e).

For a better comprehension of complex impedance behavior, an equivalent circuit model will be used. This electrical circuit is based on RC and LRC elements, following the same procedure as in other studies dealing with nanoparticle-based composites [29,30]. The tunneling mechanisms are modeled by a parallel R-C element, where R corresponds to the tunneling resistance, R_{tunnel}, modeled by G. Simmons [43], denoting the hopping conduction between neighboring nanoparticles; and C corresponds to the insulating medium. On the other hand, the contact and intrinsic mechanisms are modeled by a series–parallel L-R-C element, where the L-R terms correspond to the intrinsic resistive-inductive behavior of the nanoparticles [44] and the capacitance regards to their micro-capacitive behavior when adding to an insulating medium [26].

However, the use of a capacitor element is only valid in ideal systems, where no energy scattering is expected. In this case, these capacitive elements are substituted by Constant Phase Elements (CPEs). They are capacitive-resistive elements whose impedance is defined as $Z = 1/(Q_0(j\omega)^n)$, where Q_0 is a frequency-independent factor related to the capacitance, and n is an exponent ranging from 0 to 1, indicating the capacitive behavior of the element. A value of n = 0 denotes a purely resistive element, while n = 1 indicates a pure capacitive element. Here, the use of CPE denotes energy scattering, as commented before, in opposition to the energy conservation of a pure capacitor [45].

Therefore, the schematics of the electrical circuit used for fitting the measurements and the correlation between the fitted and the measured data are shown in the solid lines of Fig. 4, where a high correlation is found, highlighting the validity of the proposed circuit for properly capturing the electrical impedance behavior of the system. Moreover, the values of the fitting parameters are summarized in Fig. 5.

Several statements can be made when analyzing the values of fitting parameters. On the one side, there is a general reduction of the electrical resistance of both intrinsic/contact and tunneling mechanisms when increasing the nanofiller content. More specifically, it is possible to analyse the evolution the electrical resistance from the percolation threshold (set as 11 wt% for CB-based and 1 wt% for GNP-based nanocomposites) to nanofiller contents widely above this threshold. The reduction of the intrinsic and contact resistance is explained because, when increasing the nanofiller content, the number of parallel pathways increases due to the higher number of contact points between adjacent nanoparticles. Moreover, the reduction of the electrical resistance associated with tunneling mechanisms decreases for the same reason as well as due to the lower interparticle distance between neighboring nanoparticles when increasing the nanofiller content, which leads to a reduction of tunneling resistance according to J.G. Simmons formula [43].

Furthermore, it can be also noticed that for pure GNP and CB nanocomposites, an increase in the nanofiller content is manifested in an increase in the ratio $R_{intrinsic}/R_{tunnel}$ as shown in Fig. 6a. This means that, at higher nanofiller contents, a higher prevalence of contact mechanisms takes place due to the presence of a more agglomerated network (Fig. 6b and c).

However, the behavior is quite more complex in the case of CB-GNP hybrid nanocomposites. First, it can be noticed that, for a fixed CB content, an increase in the GNP content leads to a drastic change in the complex impedance response. More specifically, the electrical impedance behavior is more like pure-CB nanocomposites when increasing the

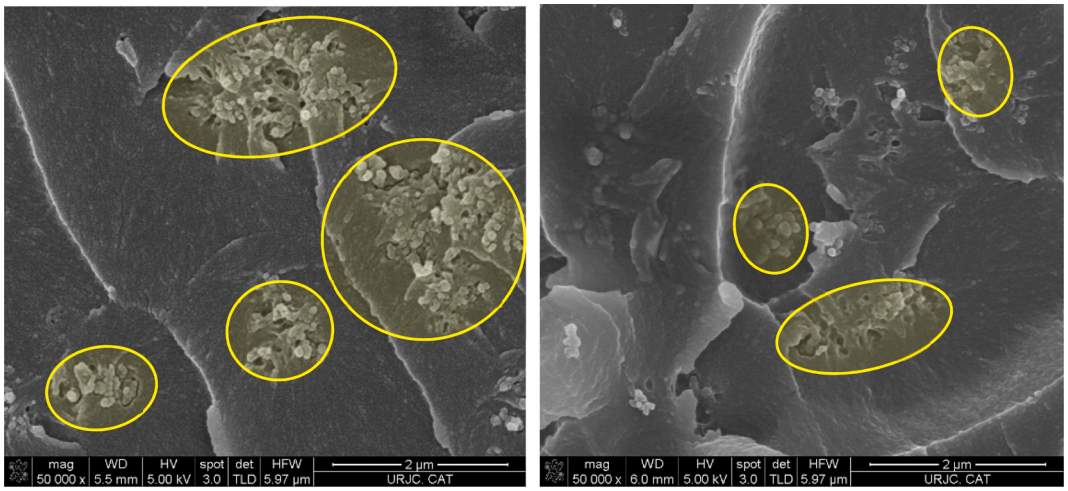

(a) (b)

Fig. 3. FEG-SEM images of (a) CB5-G1 and (c) CB3-G1 samples where the CB agglomerates are highlighted in yellow circles.

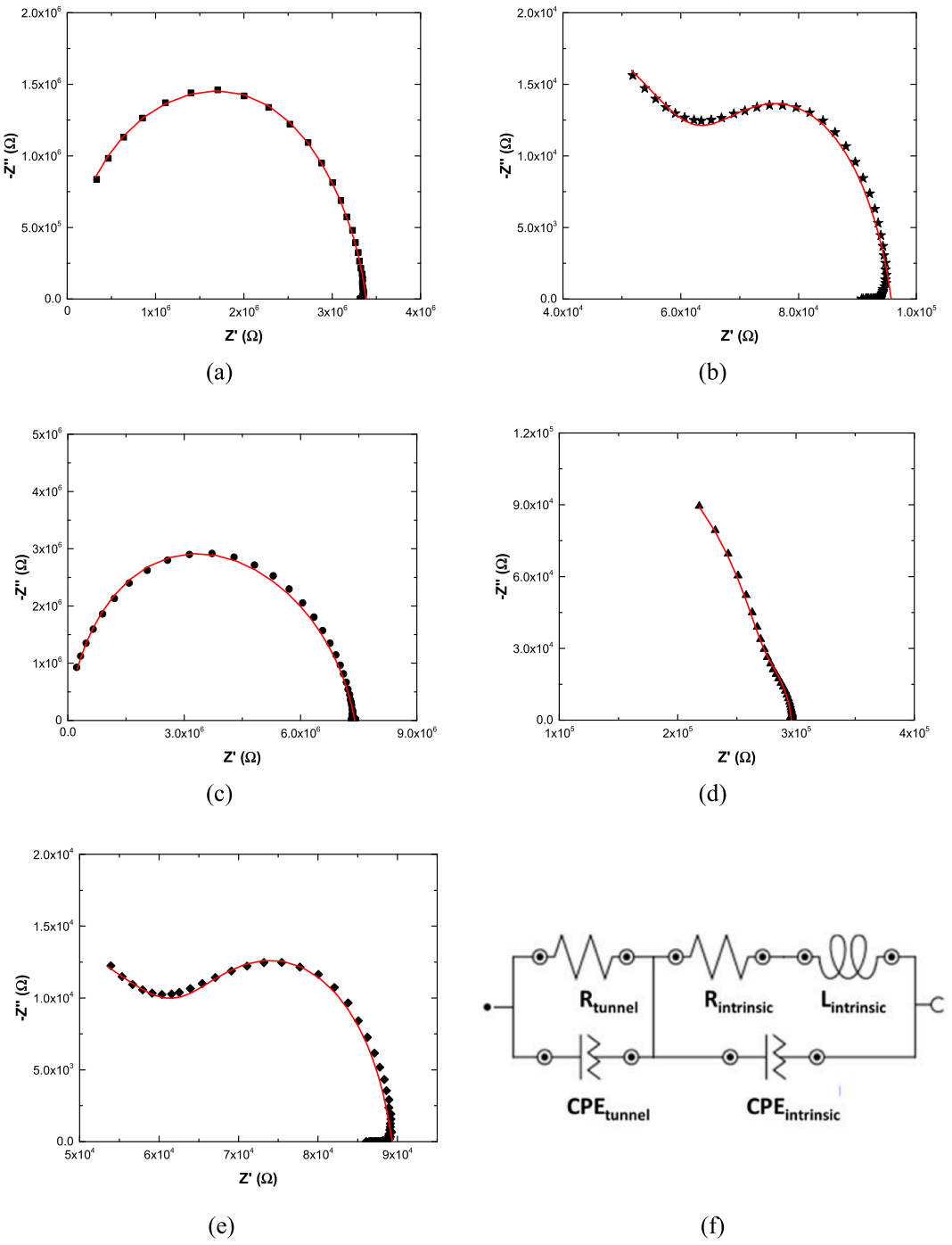

Fig. 4. Nyquist plots (−Z'' versus Z') of (a) G1, (b) CB11, (c) CB5-G1, (d) CB5-G2 and (e) CB5-G3 nanocomposites, where the black dots denote the experimental results and the solid lines the fitting with (f) the equivalent circuit (the rest of Nyquist plots can be found in Fig. S2).

GNP content. This behavior can be contradictory at first sight but can be explained by analyzing the electrical network formed within the nanocomposite. At low GNP contents, the nanoplatelets are isolated from the CBs (Fig. 6d), whereas at higher GNP contents, many connections between the nanoplatelets and the CBs are formed (Fig. 6e and f).

By analyzing the values of $R_{intrinsic}/R_{tunnel}$, it can be observed that, in the case of 5 wt% CB hybrid nanocomposites, there is a lower prevalence of contact mechanisms for CB5-G2 samples, whereas in the case of 3 wt % CB hybrid ones, CB3-G3 samples presented a lower prevalence of contact mechanisms. This effect can be explained by how the electrical percolating network is formed in these hybrid nanocomposites.

In this regard, for better comprehension, schematics of electrical transport mechanisms for CB-GNP hybrid nanocomposites are shown in Fig. 7. It can be stated that, at low GNP/CB ratios, the electrical transport mechanisms take place mainly through the percolating GNP network, whereas the CB domains remain almost isolated from the electrical network (Fig. 7a). Here, it is important to point out that the CB content (3 or 5 wt%) is far below the percolation threshold of the pure-CB (between 8 and 11 wt%) so these domains are not able to form a percolating network by themselves. By increasing the GNP content, several connections between the percolating GNP network and the isolated CB domains are created, and the electrical transport mechanisms occur through the GNPs and the CB domains (Fig. 7b). At this point, the electrical percolation takes place through both GNPs and CBs from the

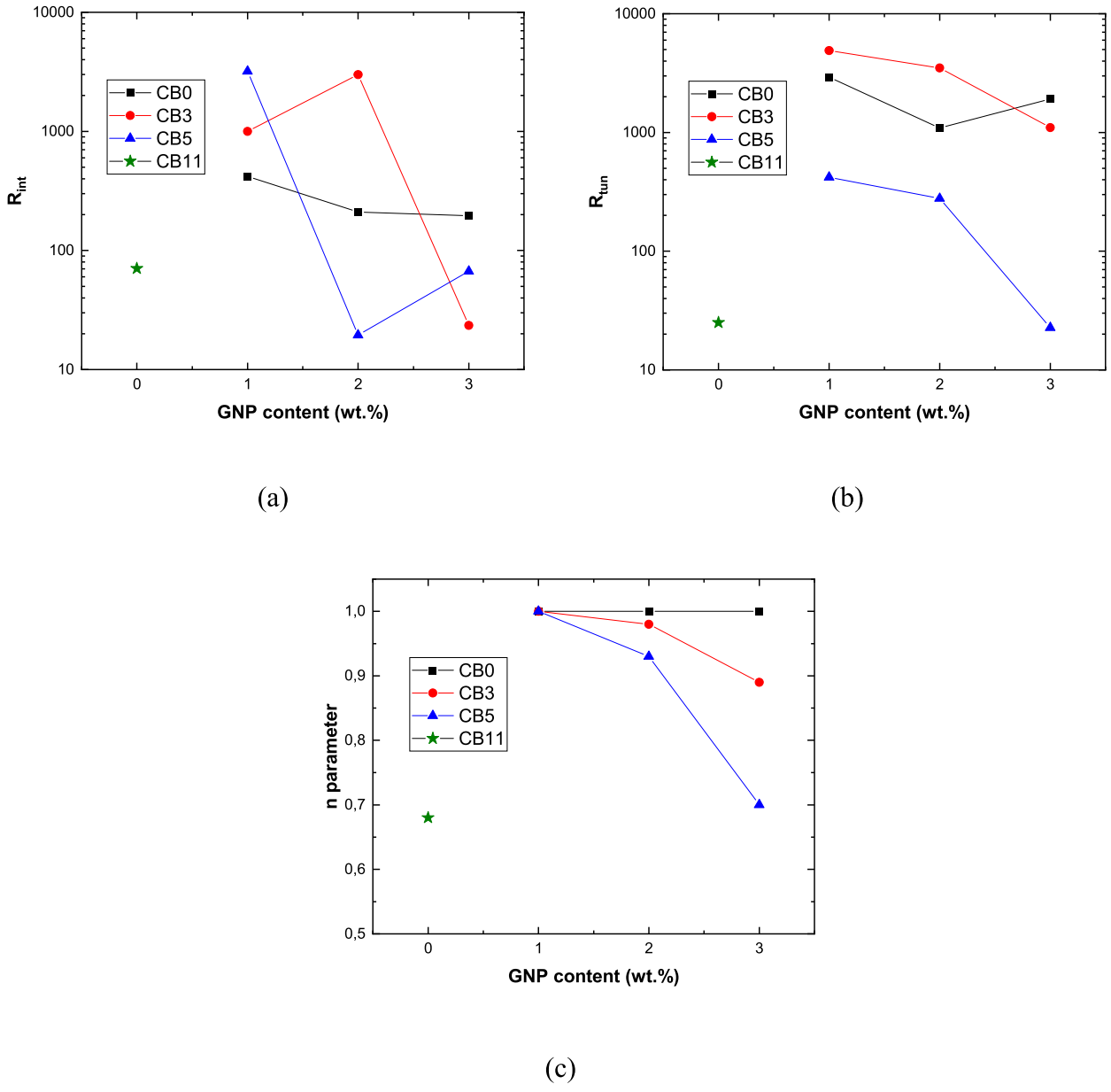

Fig. 5. Values of the fitting parameters for (a) R_{int}, (b) R_{tun} and (c) *n* parameter of intrinsic term (the rest of the fitting values are given in Table S2).

connections created between them (Fig. 6e), and, thus, tunneling mechanisms are prevalent, as observed in the graph of Fig. 6a. Finally, at higher GNP contents, these connections between the CBs and the GNPs are much more prevalent (Fig. 6f) and the electrical transport mechanisms take place mainly through the CB domains (Fig. 7c) as they present a lower contact and intrinsic resistance due to their 0D nature when compared to the 2D nanoplatelets, as well as due to their highly aggregated state. For this reason, a drastic increase of $R_{intrinsic}/R_{tunnel}$ is noticed (Fig. 6a), as the aggregated areas are the most relevant for the electrical transport in this type of material. In the case of 3 wt% CB hybrid nanocomposites, the interconnections between GNPs and CBs are formed at higher GNP contents, as the CB domains are much more isolated, and, thus, the decrease of $R_{intrinsic}/R_{tunnel}$ is noticed at 3 wt% GNPs, indicating that, at this point, a double-percolation transport between both the GNP and CB domains is created.

Apart from the electrical transport mechanisms in CB-GNP nanocomposites, the analysis of fitting parameters also sheds light on how ideal this transport between nanoparticles is. Particularly, it can be observed that the value of the *n* parameter of the CPE element associated with intrinsic and contact mechanisms is much lower in the case of CBs (0.73 for 11 wt% CB nanocomposite) than in the case of GNPs (around 1 in every case). As commented before, a lower *n* value denotes a higher resistive behavior which implies a more significant energy scattering. In this regard, it can be stated that the contact between the CBs is more irregular than in the case of GNPs (Fig. 8) as the nanoparticles are not totally in contact throughout a plane but in a single point (highlighted in Fig. 8) and, therefore, it would explain the higher scattering effects and the less ideal behavior of the system.

Furthermore, in the case of CB-GNP hybrid nanocomposites, a decrease of the *n* parameter is observed for a fixed CB content when increasing the GNP one. This is in good agreement with the previous observations highlighting the prevalence of CB transport mechanisms when increasing the GNP amount, due to the connections created between both nanofillers. This reduction of the *n* parameter is more prevalent for 5 wt% CB hybrid nanocomposites than for 3 wt% CB ones, as the electrical transport mechanisms through the CBs once inside the percolating network, are more relevant in the first case.

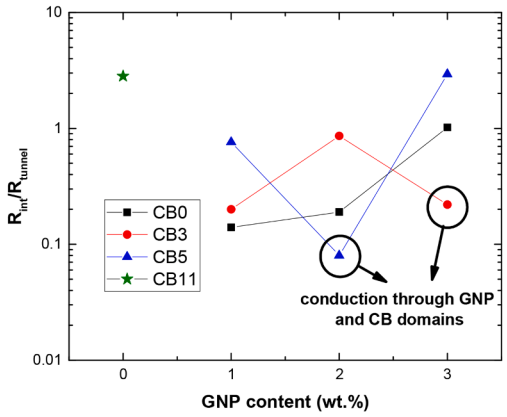

(a)

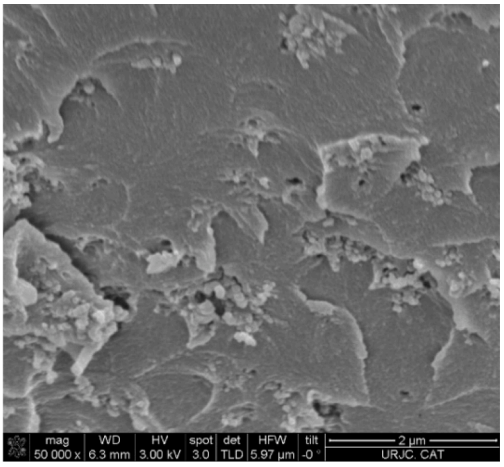

(b)

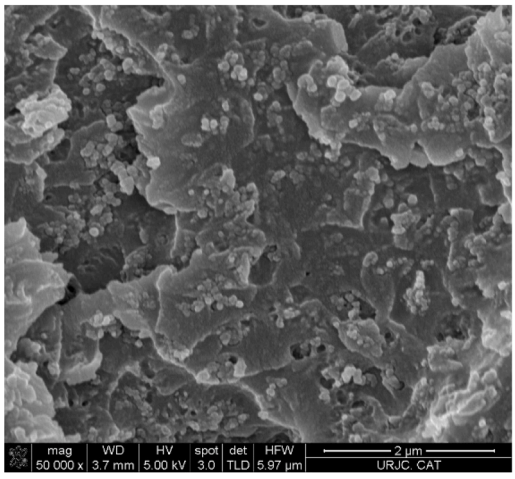

(c)

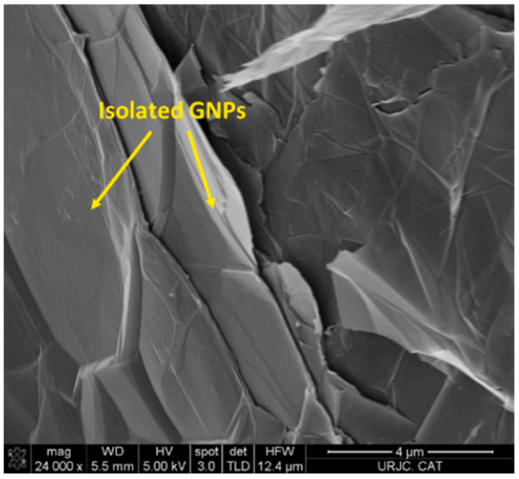

(d)

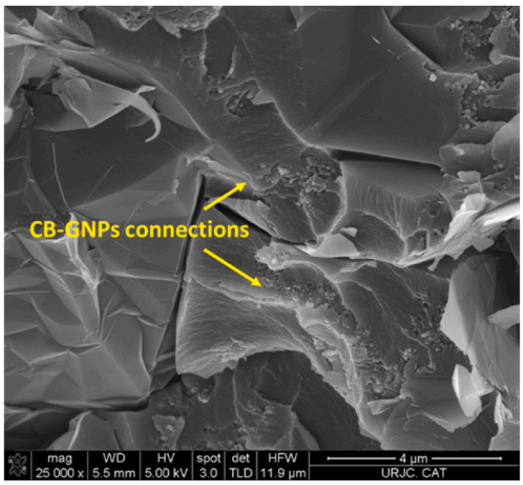

(e)

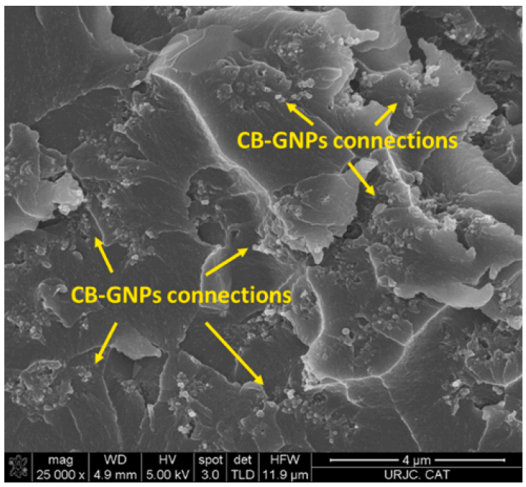

(f)

Fig. 6. (a) Values of $R_{intrinsic}/R_{tunnel}$ from the fitting parameters using the equivalent circuit of Fig. 5a and FEG-SEM images of (b) CB5, (c) CB11, (d) CB5-G1, (e) CB5-G2, and (f) CB5-G3 nanocomposites.

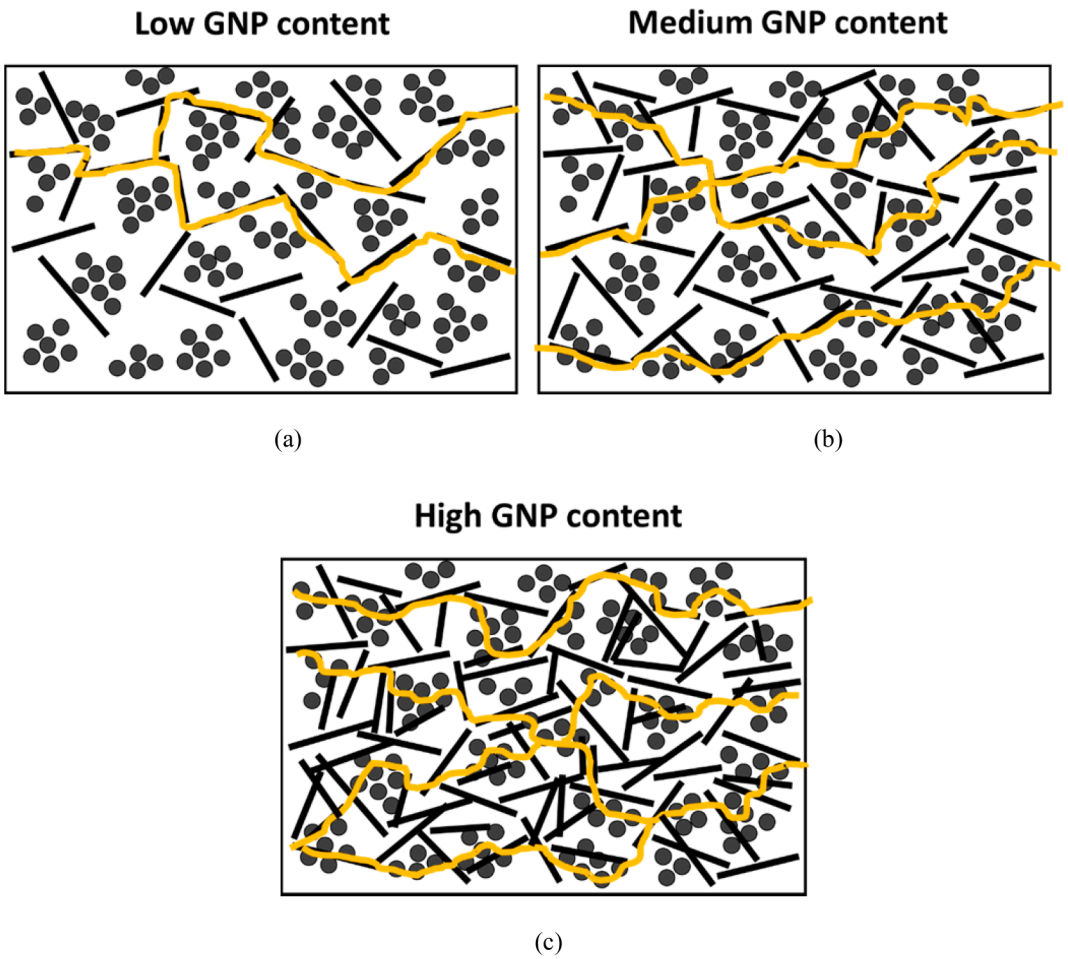

Fig. 7. Schematics of electrical transport for (a) low, (b) medium and (c) high GNP-filled hybrid composites based on the electrical impedance analysis, where the orange lines denote the preferential electrical pathways.

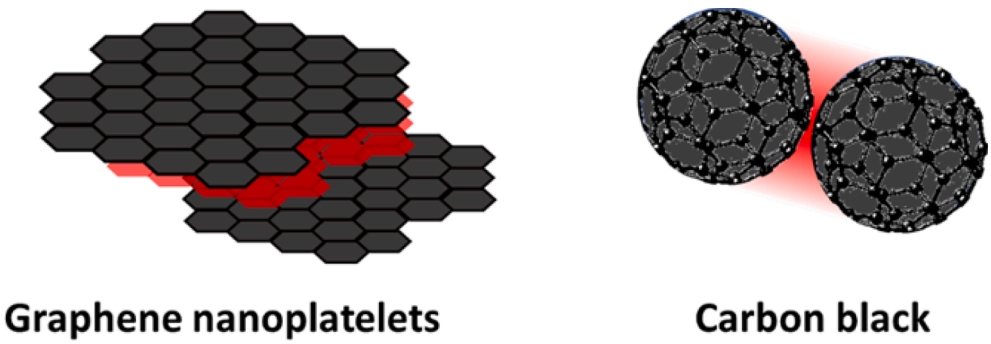

Fig. 8. Contact mechanisms between adjacent GNPs and CBs (marked in red).

3.3. Doble percolation modeling

The analysis of fitting parameters from Fig. 5 can give detailed information about the predominance of some electrical transport mechanisms in hybrid CB-GNP nanocomposites, as commented before. In this way, it is possible to understand how electrical percolation takes place in these materials.

In this sense, a double percolation threshold can be determined for each constituent (CB and GNP). This double percolation threshold concept was first coined by M. Sumita et al. [46] for the dispersion of nanofillers inside polymer blends. In particular, the effective volume fraction of nanofiller in co-continuous morphologies can be estimated from the volume of the phase in which the nanofiller is localized and its real volume fraction [31,32]. Here, a novel concept is proposed.

For a CB-GNP hybrid nanocomposite, the percolation threshold of the system can be determined from the percolation threshold of the CB constituent, the GNP one, or a mix between both percolation thresholds. More specifically, for a fixed CB content, i.e., 5 wt%, at low GNP contents (1 wt%) the electrical transport mechanisms take place through the GNP nanofillers, as they form an electrical percolating network. That is, the electrical percolation threshold of the system is the same as the pure-GNP nanocomposite, which is defined as ϕ_{Gc}. When increasing the GNP content to 2 wt% a co-continuous electrical network is formed between the GNPs and the CBs. Here, both the GNPs and the CBs form electrical

percolating networks, as observed before. The effective volume fraction of CBs, ϕ_{CBeff}, can be calculated from this expression, which is inspired by that proposed in co-continuous blends with nanofillers [31]:

$$\phi_{CBeff} = \frac{\phi_{CB}}{(1-\phi_{Ginf})} \quad (3)$$

Where ϕ_{CB} is the CB volume fraction and ϕ_{Ginf} the volume of influence of the GNPs. This volume of influence depends on how GNPs are dispersed through the material and denotes the area affected by the electrical transport mechanisms of these nanoparticles (gray areas of schematics of Fig. 9). Therefore, the volume fraction of the phase in which the CBs are localized is $(1-\phi_{Ginf})$.

The volume of influence of the GNPs can be easily calculated in our case supposing that, with 2 wt% GNPs, the 5 wt% CB network forms a percolating one and, thus, ϕ_{CBeff} coincides with the percolation threshold determined experimentally. Here, from the DC measurements, the percolation threshold was found to be between 8 and 11 wt% CB, so it will be considered at an intermediate weight fraction, that is $\phi_{CBc} = 10$ wt%.

Finally, at higher GNP contents (3 wt%), the electrical transport mechanisms occur mainly through the CB areas, and, therefore, the electrical percolation threshold is more like that from the pure-CB nanocomposite.

With all these assumptions, it is possible to estimate the value of the electrical conductivity for every case by using the following expressions, based on the classical percolation theory with scaling power law [47]:

$$\sigma = \sigma_{0G}(\phi_G - \phi_{Gc})^t when \phi_{CBeff} \ll \phi_{CBc}$$

$$\sigma = a \bullet \sigma_{0G}(\phi_G - \phi_{Gc})^t + b \bullet \sigma_{0CB}(\phi_{CBeff} - \phi_{CBc})^t when \phi_{CBeff} \ \phi_{CBc} \quad (4)$$

$$\sigma = \sigma_{0CB}(\phi_{CBeff} - \phi_{CBc})^t when \phi_{CBeff} \gg \phi_{CBc}$$

Being σ_{0G} and σ_{0CB} two pre-exponential factors for GNPs and CBs, respectively, that depend on the intrinsic electrical conductivity of the nanofillers and their geometry (i.e. aspect ratio) [48]; t an exponent which ranges typically from 1.3 to 2, both obtained from fitting the DC conductivity of pure-GNP and CB materials; and a and b, two parameters ranging from 0 to 1 ($a + b = 1$), which depend on the prevalence of GNP or CB mechanisms.

In particular, the values of a and b can be estimated from the fitting parameters of the complex impedance of Fig. 5 and Table S2 by using the following expressions:

$$b = \frac{(n_{GNP} - n_{CB/GNP})}{(n_{GNP} - n_{CB})} \quad a = 1 - b \quad (5)$$

Where n_{GNP} and n_{CB} are the values of the n parameter for pure-GNP and CB, respectively (1 and 0.68 from Table S2) and $n_{CB/GNP}$ the actual n value of the hybrid nanocomposite.

In this sense, Fig. 10 shows the measured and fitted data using

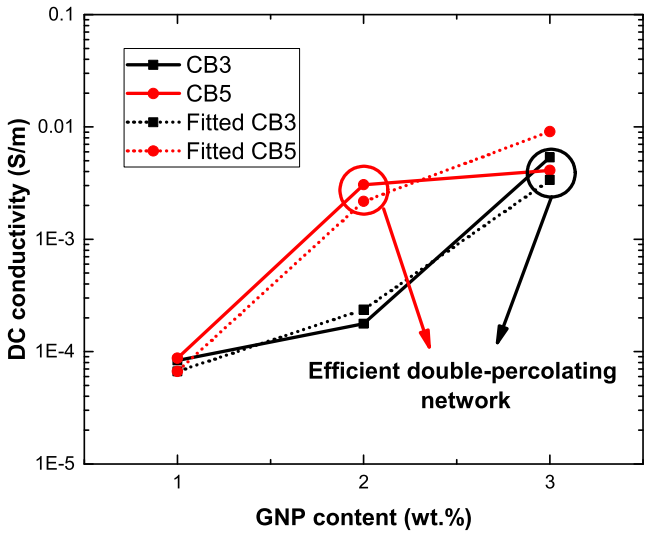

Fig. 10. Values of the DC conductivity by using Equations (4) and (5) for the hybrid CB-GNP nanocomposites.

Equations (4) and (5) of the DC conductivity (σ_0 values). Here, a good agreement between the theoretical predictions and the experimental results is found. More specifically, the model properly captures the drastic increase of the electrical conductivity for CB3-G3 and CB5-G2 samples as, at these conditions, an efficient double-percolating network is created through the GNP and CB domains, where the electrical transport is dominated by the tunneling connections between the GNPs and the CBs. The slight differences observed between the experimental and the predicted values at the highest nanofiller content (CB5-G3) may be attributed to the presence of a very highly aggregated network, as observed before. Here, the percolating networks are not so effective, and the model may overestimate the electrical conductivity of the system. Anyway, the differences found are not so prevalent and, therefore, it can be stated that the proposed model properly captures the main electrical transport mechanisms in a hybrid CB-GNP nanocomposite from the complex impedance measurements and the analysis of the equivalent circuits.

4. Conclusions

The analysis of electrical transport mechanisms in hybrid CB-GNP nanocomposites has been carried out through DC and EIS measurements.

From DC measurements, it has been observed that the samples with a low nanofiller content do not follow an ohmic behavior, due to the matrix-dominated electrical mechanisms. However, at high nanofiller contents, the I-V curves follow a linear relationship because of the

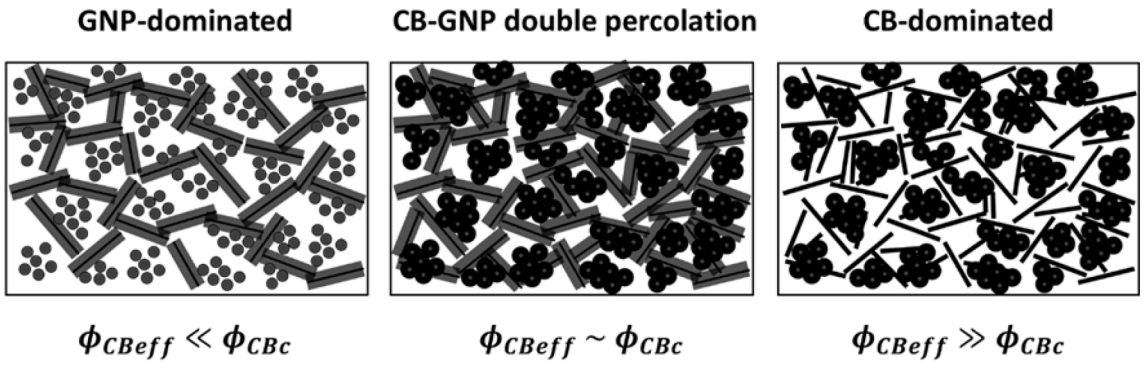

Fig. 9. Schematics of electrical percolating networks for CB-GNP nanocomposites as a function of CB-GNP ratio.

prevalence of contact mechanisms and the lower temperature-dependent electrical behavior.

From EIS analysis, it is possible to know the electrical transport mechanisms in a more detailed way by adjusting the measured data to an equivalent electrical circuit. This circuit is composed of a series of LRC, for contact and intrinsic mechanisms between adjacent nanoparticles, and RC, for tunneling transport between neighboring ones. Here, the capacitances are substituted by CPEs because of the non-ideal behavior of the system, especially in the interconnections between CBs.

The analysis of fitting parameters showed a prevalence of GNP transport mechanisms at high CB/GNP ratios as the GNPs form a percolating network that is not able to connect the isolated CB domains. When increasing the GNP content, some connections between the percolated GNP network and the CBs are created and, thus, a double-percolating network is formed. Finally, at higher GNP contents, the GNPs can connect all the main CB domains, and, thus, the electrical transport mechanisms are CB-dominated.

Therefore, a double-percolation model based on the classical percolation theory and the analysis of electrical transport mechanisms by DC and EIS measurements has been proposed. This double-percolation model properly fits the electrical measurements. In this regard, it is a significant progress in comparison with the current models, which are based on complex numerical simulations by providing a simple but effective analytical approach that properly explains the main electrical transport mechanisms in hybrid CB-GNP nanocomposites by correlating the value of the *n* parameter with the prevalence of CB or GNP-dominated electrical transport mechanisms with a double percolation approach. It would be, thus, very promising for the creation of hybrid nanocomposites with tunable properties.

CRediT authorship contribution statement

X.F. Sánchez-Romate: Writing – original draft, Methodology, Formal analysis, Conceptualization. **A. Jiménez-Suárez:** Writing – review & editing, Supervision, Conceptualization. **J.M. Sanz-Ayet:** Formal analysis, Methodology. **V. García-Martínez:** Conceptualization, Methodology. **M.R. Gude:** Conceptualization, Writing – review & editing. **S.G. Prolongo:** Funding acquisition, Writing – review & editing.

Declaration of competing interest

The authors declare that they have no known competing financial interests or personal relationships that could have appeared to influence the work reported in this paper.

Data availability

Data will be made available on request.

Acknowledgements

This work was supported by the Agencia Estatal de Investigación of Spanish Government [PROJECT SMART-ECOCOMP PID2022-138496OB-I00] and PROJECT TEMACON (HUBS 49/520635.9/18)].

Appendix A. Supplementary data

Supplementary data to this article can be found online at https://doi.org/10.1016/j.compositesa.2024.108273.

References

[1] Yu MF, Lourie O, Dyer MJ, Moloni K, Kelly TF, Ruoff RS. Strength and breaking mechanism of multiwalled carbon nanotubes under tensile load. Science 2000;287:637–40.
[2] Ghaleb ZA, Mariatti M, Ariff ZM. Properties of graphene nanopowder and multi-walled carbon nanotube-filled epoxy thin-film nanocomposites for electronic applications: The effect of sonication time and filler loading. Composites Part A-Applied Science and Manufacturing 2014;58:77–83.
[3] Oh JY, Jun GH, Jin S, Ryu HJ, Hong SH. Enhanced electrical networks of stretchable conductors with small fraction of carbon nanotube/graphene hybrid fillers. ACS Appl Mater Interfaces 2016;8:3319–25.
[4] Safdari M, Al-Haik MS. Synergistic electrical and thermal transport properties of hybrid polymeric nanocomposites based on carbon nanotubes and graphite nanoplatelets. Carbon 2013;64:111–21.
[5] Ma P, Liu M, Zhang H, Wang S, Wang R, Wang K, et al. Enhanced electrical conductivity of nanocomposites containing hybrid fillers of carbon nanotubes and carbon black. ACS Appl Mater Interfaces 2009;1:1090–6.
[6] Song P, Song J, Zhang Y. Stretchable conductor based on carbon nanotube/carbon black silicone rubber nanocomposites with highly mechanical, electrical properties and strain sensitivity. Compos B Eng 2020;191:107979.
[7] Xiang D, Zhang X, Harkin-Jones E, Zhu W, Zhou Z, Shen Y, et al. Synergistic effects of hybrid conductive nanofillers on the performance of 3D printed highly elastic strain sensors. Compos A Appl Sci Manuf 2020;129:105730.
[8] Sánchez-Romate XF, Jiménez-Suárez A, Campo M, Ureña A, Prolongo SG. Electrical Properties and Strain Sensing Mechanisms in Hybrid Graphene Nanoplatelet/Carbon Nanotube Nanocomposites. Sensors 2021;21:5530.
[9] Li J, Ma PC, Chow WS, To CK, Tang BZ, Kim J. Correlations between percolation threshold, dispersion state, and aspect ratio of carbon nanotubes. Adv Funct Mater 2007;17:3207–15.
[10] Sánchez-Romate XF, Artigas J, Jiménez-Suárez A, Sánchez M, Güemes A, Ureña A. Critical parameters of carbon nanotube reinforced composites for structural health monitoring applications: Empirical results versus theoretical predictions. Composites Sci Technol 2019;171:44–53.
[11] Haghgoo M, Ansari R, Hassanzadeh-Aghdam MK, Jang S, Nankali M. Simulation of the role of agglomerations in the tunneling conductivity of polymer/carbon nanotube piezoresistive strain sensors. Composites Sci Technol 2023;243:110242.
[12] Haghgoo M, Ansari R, Kazem Hassanzadeh-Aghdam M, Tian L, Nankali M. Analytical formulation of the piezoresistive behavior of carbon nanotube polymer nanocomposites: The effect of temperature on strain sensing performance. Compos A Appl Sci Manuf 2022;163:107244.
[13] Mazaheri M, Payandehpeyman J, Khamehchi M. A developed theoretical model for effective electrical conductivity and percolation behavior of polymer-graphene nanocomposites with various exfoliated filleted nanoplatelets. Carbon 2020;169:264–75.
[14] Arun DI, Chakravarthy P, Girish BS, Kumar KS, Santhosh B. Experimental and Monte Carlo simulation studies on percolation behaviour of a shape memory polyurethane carbon black nanocomposite. Smart Mater Struct 2019;28:055010.
[15] Taherian R. Experimental and analytical model for the electrical conductivity of polymer-based nanocomposites. Composites Sci Technol 2016;123:17–31.
[16] Haghgoo M, Ansari R, Hassanzadeh-Aghdam MK. Prediction of electrical conductivity of carbon fiber-carbon nanotube-reinforced polymer hybrid composites. Compos B Eng 2019;167:728–35.
[17] Haghgoo M, Ansari R, Kazem Hassanzadeh-Aghdam M, Jang S, Nankali M. Analytical modeling of synergistic carbon nanotube/carbon black effects on the sensitivity of nanocomposite strain sensors. Compos A Appl Sci Manuf 2023;173:107711.
[18] Haghgoo M, Ansari R, Hassanzadeh-Aghdam MK. Prediction of piezoresistive sensitivity and percolation probability of synergetic CNT-GNP conductive network composite. Sens Actuators, A 2022;336:113414.
[19] Liu W, Liu Z, Guo Z, Xie W, Tang A, Huang G. A computational model for characterizing electrical properties of flexible polymer composite filled with CNT/GNP nanoparticles. Mater Today Commun 2022;32:104177.
[20] Haghgoo M, Ansari R, Hassanzadeh-Aghdam MK. Monte Carlo analytical-geometrical simulation of piezoresistivity and electrical conductivity of polymeric nanocomposites filled with hybrid carbon nanotubes/graphene nanoplatelets. Compos A Appl Sci Manuf 2022;152:106716.
[21] Haghgoo M, Ansari R, Hassanzadeh-Aghdam MK, Nankali M. Analytical formulation for electrical conductivity and percolation threshold of epoxy multiscale nanocomposites reinforced with chopped carbon fibers and wavy carbon nanotubes considering tunneling resistivity. Compos A Appl Sci Manuf 2019;126:105616.
[22] Sun Y, Bao H, Guo Z, Yu J. Modeling of the electrical percolation of mixed carbon fillers in polymer-based composites. Macromolecules 2009;42:459–63.
[23] Xiong Z, Zhang B, Wang L, Yu J, Guo Z. Modeling the electrical percolation of mixed carbon fillers in polymer blends. Carbon 2014;70:233–40.
[24] Ke K, Yue L, Shao H, Yang M, Yang W, Manas-Zloczower I. Boosting electrical and piezoresistive properties of polymer nanocomposites via hybrid carbon fillers: A review. Carbon 2021;173:1020–40.
[25] Sumfleth J, Adroher XC, Schulte K. Synergistic effects in network formation and electrical properties of hybrid epoxy nanocomposites containing multi-wall carbon nanotubes and carbon black. J Mater Sci 2009;44:3241–7.
[26] Mergen ÖB, Umut E, Arda E, Kara S. A comparative study on the AC/DC conductivity, dielectric and optical properties of polystyrene/graphene nanoplatelets (PS/GNP) and multi-walled carbon nanotube (PS/MWCNT) nanocomposites. Polym Test 2020;90:106682.
[27] Guillet J, Valdez-Nava Z, Golzio M, Flahaut E. Electrical properties of double-wall carbon nanotubes nanocomposite hydrogels. Carbon 2019;146:542–8.
[28] Can-Ortiz A, Abot JL, Avilés F. Electrical characterization of carbon-based fibers and their application for sensing relaxation-induced piezoresistivity in polymer composites. Carbon 2019;145:119–30.

[29] Tallman TN, Hassan H. A network-centric perspective on the microscale mechanisms of complex impedance in carbon nanofiber-modified epoxy. Composites Sci Technol 2019;181:107669.
[30] Bosque Ad, Sánchez-Romate XF, Sánchez M, Ureña A. Ultrasensitive and highly stretchable sensors for human motion monitoring made of graphene reinforced polydimethylsiloxane: Electromechanical and complex impedance sensing performance. Carbon 2022;192:234–48.
[31] Mun SC, Kim MJ, Cobos M, Gu L, Macosko CW. Strategies for interfacial localization of graphene/polyethylene-based cocontinuous blends for electrical percolation. AIChE J 2019;65:e16579.
[32] Khan T, Irfan MS, Ali M, Dong Y, Ramakrishna S, Umer R. Insights to low electrical percolation thresholds of carbon-based polypropylene nanocomposites. Carbon 2021;176:602–31.
[33] Sánchez-Romate XF, Saiz V, Jiménez-Suárez A, Campo M, Ureña A. The role of graphene interactions and geometry on thermal and electrical properties of epoxy nanocomposites: A theoretical to experimental approach. Polym Test 2020;90:106638.
[34] Jouni M, Faure-Vincent J, Fedorko P, Djurado D, Boiteux G, Massardier V. Charge carrier transport and low electrical percolation threshold in multiwalled carbon nanotube polymer nanocomposites. Carbon 2014;76:10–8.
[35] Rajukumar LP, Belmonte M, Slimak JE, Elías AL, Cruz-Silva E, Perea-López N, et al. 3D nanocomposites of covalently interconnected multiwalled carbon nanotubes with SiC with enhanced thermal and electrical properties. Adv Funct Mater 2015;25:4985–93.
[36] Sánchez-Romate XF, Sans A, Jiménez-Suárez A, Prolongo SG. The addition of graphene nanoplatelets into epoxy/polycaprolactone composites for autonomous self-healing activation by Joule's heating effect. Composites Sci Technol 2021;213:108950.
[37] Pelech I, Kaczmarek A, Pelech R. Current-Voltage Characteristics of the Composites Based on Epoxy Resin and Carbon Nanotubes. J Nanomater 2015;2015:405345.
[38] Loeblein M, Bolker A, Ngoh ZL, Li L, Wallach E, Tsang SH, et al. Novel timed and self-resistive heating shape memory polymer hybrid for large area and energy efficient application. Carbon 2018;139:626–34.
[39] Sánchez-Romate XF, Gutiérrez R, Cortés A, Jiménez-Suárez A, Prolongo SG. Multifunctional coatings based on GNP/epoxy systems: Strain sensing mechanisms and Joule's heating capabilities for de-icing applications. Prog Org Coat 2022;167:106829.
[40] Ning W, Wang Z, Liu P, Zhou D, Yang S, Wang J, et al. Multifunctional super-aligned carbon nanotube/polyimide composite film heaters and actuators. Carbon 2018;139:1136–43.
[41] Guan R, Zou F, Li D, Yao Y. A high-thermal-stability, fully spray coated multilayer thin-film graphene/polyamide-imide nanocomposite strain sensor for acquiring high-frequency ultrasonic waves. Composites Sci Technol 2022;227:109628.
[42] Cardoso P, Silva J, Agostinho Moreira J, Klosterman D, van Hattum FWJ, Simoes R, et al. Temperature dependence of the electrical conductivity of vapor grown carbon nanofiber/epoxy composites with different filler dispersion levels. Phys Lett A 2012;376:3290–4.
[43] Simmons JG. Generalized formula for the electric tunnel effect between similar electrodes separated by a thin insulating film. J Appl Phys 1963;34:1793–803.
[44] Kang J, Matsumoto Y, Li X, Jiang J, Xie X, Kawamoto K, et al. On-chip intercalated-graphene inductors for next-generation radio frequency electronics. Nat Electron 2018;1:46–51.
[45] Lasia A. The origin of the constant phase element. The Journal of Physical Chemistry Letters 2022;13:580–9.
[46] Sumita M, Sakata K, Asai S, Miyasaka K, Nakagawa H. Dispersion of fillers and the electrical conductivity of polymer blends filled with carbon black. Polym Bull 1991;25:265–71.
[47] Blighe FM, Hernandez YR, Blau WJ, Coleman JN. Observation of Percolation-like Scaling-Far from the Percolation Threshold–in High Volume Fraction, High Conductivity Polymer-Nanotube Composite Films. Adv Mater 2007;19:4443–7.
[48] Shimamura Y, Yasuoka T, Todoroki A. Strain sensing by using piezoresistivity of carbon nanotube/flexible-epoxy composite. In: Proceedings of the 16th International Conference on Composite Materials, Vol. 224503; 2007.